Date October 18, 2019
Our reference WES-2019-50
Contact person J.A. Frederik
Telephone/fax +31 (0)15 27 85623 / n/a
E-mail J.A.Frederik@TUDelft.nl
Subject Author's response

Delft University of Technology

Delft Center for Systems and Control

Address
Mekelweg 2 (3ME building)
2628 CD Delft
The Netherlands

www.dcsc.tudelft.nl

Referees
Wind Energy Science Discussion

Dear Referees,

First of all, the authors would like to thank the reviewers for their positive and constructive feedback. We believe that the comments have helped us to further improve the quality of the paper. In our attempt to account for the comments, we have revised different aspects of the paper. The objective of this document is to respond to the points raised by the reviewers and to provide a detailed overview of the changes made to the paper. In the subsequent sections, we will respond to the review report provided by each of the reviewers.

Yours sincerely,

Joeri Frederik

Enclosure(s): Response to comments of Anonymous Referee #1
Response to comments of Johan Meyers
Response to comments of Anonymous Referee #3
Response to comments of Anonymous Referee #4

Response to comments of Anonymous Referee #1

- The paper is well presented and well argued, and adds valuable contributions to the literature, including a first analysis of loads in dynamic induction control as well as a wind tunnel study validating the approach. The figures and descriptions are good, and the paper is very direct to understand.

  The authors would like to thank the referee for the positive feedback.

- Mostly minor comments follow below. Main over-arching comment is really a question to propose be considered in the next version of the paper. Fig 9 shows very small effect on turbine 3. Is this to be expected? In completing this review, I re-read "Towards practical dynamic induction control of wind farms: analysis of optimally controlled windfarm boundary layers and sinusoidal induction control of first-row turbines and found this passage: Figure 8 illustrates that the first-row optimized thrust coefficient also results in a significant power increase in the third row, which is not observed using the sinusoidal thrust strategy. Furthermore, the analysis of the modified control cases in Fig. 11 proves that the first-row controls are also partially synchronized with the flow. This shows that other mechanisms, dependent on specific flow events for increasing windfarm power, are at play as well. Even though the application of regression algorithms in an attempt to link turbine actions to low-dimensional flow measurements (e.g., local velocity, shear and kinetic energy) has been unsuccessful thus far, similar analysis based upon more complex flow features (e.g., vorticity structures, high-speed turbulent streaks, or downdrafts) might be more promising. This requires further optimal control simulations over an extended time, as the total control time horizon of 30 min in the current dataset is insufficient for robust statistics in this kind of analysis. This is an important remaining challenge to be addressed in future research. As well as this from the conclusion of the same paper: Although the first-row sinusoidal control led to a robust increase in total power for a reduced-size 44 wind farm, a full-scale test indicated that downstream turbine activity is required to obtain increased power at larger farm scales. It was also shown that the simple sinusoidal strategy does not lead to increased power extraction when applied to downstream intermediate turbines. Identifying the mechanisms for power increase in these turbines hence remains an important open research question. My reading is that yes, these results do confirm this, the third turbine is not expected to increase in power unless (if I understand correctly) 1. The first turbine pursues a non-sinusoidal DIC or 2. The second turbine performs DIC additionally Do you agree? Are there plans to try any DIC on the second turbine etc?

Figures 9-11 in the paper show that, in the wind tunnel, turbine 3 does in fact have a slightly increased power production when periodic DIC is applied on turbine 1. This gain is very small - much smaller than the gain obtained at turbine 2 - but as Figure 10 shows, it is in fact significant. Therefore, the claim that *no* power increase at turbine 3 is expected with periodic DIC is therefore not supported by the data presented in this paper. However, to address this point more specifically in the paper, both in the analysis in Section 6.1 and in the Conclusions, it will be stressed that the majority of the gain in power production is obtained at turbine 2. With regards to periodic DIC on the second turbine: we have in fact executed wind tunnel experiments with periodic DIC on both the first and the second turbine. However, the results of these experiments are as of yet inconclusive, which is why they are not included in this paper. Future research in this topic would definitely be of interest to us, although there are no direct plans for this. For completeness, this research direction is added to the future research opportunities in Section 7.

- Small Comments: Fig 1 could use a more descriptive labeling/caption, its not clear what each of the lines represent

  A more descriptive caption is added to Figure 1 to explain more elaborately what is shown in this figure: *A schematic representation of a wind turbine in flow field, showing the working principles of static (a) and dynamic induction control (b). On the top, the turbine is simplified as a rotor disk, and its streamtube - the area where the wind speed is affected by the turbine settings - is depicted. The force F_T exerted on the wind is shown for different induction settings, where red depicts greedy control, orange and yellow arbitrary static derating settings, and green periodic DIC. The bottom figures show the corresponding wind velocity profiles, with respect to inflow velocity U_∞, as a function of the distance from the turbine. The area highlighted in blue is where a downstream turbine is typically located.*

- DTU 5 MW turbine (Jonkman et al., 2009), shouldnt that be NREL? 5MW (based on reference provided)

  The referee is absolutely right. This erratum has been corrected as suggested.

- Table 1, for experiments the control input is Beta, but amplitude is specified in Ct? (Now I see this is explained later in the text, but might be good to ensure the explanation is indicated in the table or indicate to the reader explanation is coming?)

  To clarify the effect of β on C_T', the following sentence is added in the caption of Table 1: *Note that the pitch amplitude $\beta = 2^\circ$ used in the simulations leads to a amplitude of approximately $C_T' = 1.5$.*

- Figure 6: This is a really useful view into the loading impacts Is there a reference for Weibull-weighted DELs? A nice idea, are they used often?

XXX

- Fig 7-8, why do the effects persist above 15 m/s? I believe this addressed in text, but could be useful to re-iterate in caption, maybe also indicate with a vertical line where the DIC would be actually shut off?

  As mentioned in the text, "The DIC was assumed to be activated for wind speeds between 3 and 25 m/s, to cover the totality of regions I-1/2, II, II-1/2 and III", which "is to be regarded as a conservative choice". When DIC is only applied in region II, the loads will of course be identical to the baseline case above rated wind speeds. To further emphasize this, a vertical line is included to indicate the rated wind speed, with the caption describing that "Typically, DIC will only be implemented at below-rated inflow velocities."

- Fig 8: seems to have an error in caption

  There is indeed an error in the caption, which has been removed.

- Section 6.2 Do you use the FLORIS model of Gebraad 2016, or the newer gaussian model of Bastankah within FLORIS? Maybe provide FLORIS version number?

  The FLORIS model with gaussian distribution as proposed by Bastankah was used. For clarity, the reference was changed to represent the version that was used in this paper.

Response to comments of Johan Meyers

- Very interesting work, which I strongly recommend for publication. I have a number of smaller comments, that should be relatively easy to incorporate in a revision.

  The authors would like to thank prof. Meyers for the kind words, and hope to address all the smaller comments to his satisfaction.

- 1. abstract: In this paper, only periodic variation, ¿ variations

  This erratum has been corrected as suggested.

- 2. Figure 1: please improve. In 1a (bottom) for clarity, please indicate levels of C_T associated with different velocity profiles. In 1b, not clear what the order is of the velocity profiles (in time or phase of the sinusoidal forcing). Also not 100% convinced that this will be the effective response is this an artists impression, or is this based on some model? Please clarify in the fig caption and text.

  To answer the final question posed by the referee: this figure is not based on some model or measurement, but rather a schematic representation of the flow through a rotor streamtube, meant only to clarify the working principle of DIC with respect to static induction control. As such, the lines do not represent specific values of C_T or U_∞. To emphasize this, a more elaborate caption has been added to this figure: *A schematic representation of a wind turbine in flow field, showing the working principles of static (a) and dynamic induction control (b). On the top, the turbine is simplified as a rotor disk, and its streamtube - the area where the wind speed is affected by the turbine settings - is depicted. The force F_T exerted on the wind is shown for different induction settings, where red depicts greedy control, orange and yellow arbitrary static derating settings, and green periodic DIC. The bottom figures show the corresponding wind velocity profiles, with respect to inflow velocity U_∞, as a function of the distance from the turbine. The area highlighted in blue is where a downstream turbine is typically located.*

- 3. In the paper, it is suggested a couple of times that CFD is performed: - Page 2: Simulations will be executed using the high-fidelity Computational Fluid Dynamics (CFD) environment SOWFA - Page 7: Once the optimal DIC parameters in terms of wake mixing have been evaluated using CFD, ... However, apart from these, CFD seems not to be really discussed... Please clarify. If you use CFD in some way, it would merit a much lengthier description (computational domain, mesh, boundary conditions, models used, some results, ...)

The CFD simulations mentioned here were removed from the paper in one of the final stages before submission. The most important reason for this was that the authors felt like the contribution of this CFD study to the already existing literature (mostly by Munters and Meyers) was limited. We therefore chose to focus on the most important scientific contributions: the load analysis and the wind tunnel experiments. All references to CFD simulations have been removed in the updated version of the manuscript.

- 4. Figure 2: how was this figure constructed (please make caption more selfcontained). Did you use the procedure described on top of page 4? Or did you use BEM, or the Cp-Lambda model, ...

  This figure was constructed using look-up tables based on data from the $G1$ turbine models. For clarity, this has been added to the caption: *Values of C_T for different types of input signals, created using a look-up table for the G1 turbine model. The thrust coefficient is shown for three different sinusoidal excitations: on C_T, on C_T' and on the collective pitch angle β, tuned such that the amplitude of C_T' is 1.5. The dashed line shows the steady-state optimal C_T.*

- 5. page 4: A region I-1/2 with constant rotor speed equal to 6 rpm extends from the cut-in speed of 4 m/s to 7 m/s. Im a bit surprised by this please double check. As far as I remember, in region 1.5 the rotor speed is increasing, and not constant.

  XXX

- 6. Table 2: for completeness, please add values for average pitch angle and amplitude of pitch oscillation

  As suggested by the referee, mean values of the average and amplitude of the pitch angle are added to Table 2.

- 7. Following up on previous point, for sake of reproducibility, it would make sense to add a detailed figure with the C_T & C_T' signal together with the pitch signal and the rotational speed signal

  As requested by the referee, such a figure has been added to Section 6. The figure shows the requested variables for the optimal low-TI case: $St = 0.31$, $A = 1$. The C_T and C_T' measurements are displayed, both filtered and unfiltered, as well as the best sinusoidal fit to this data. Furthermore, the pitch excitation and the rotor speed is given, with the latter also compared to the baseline case.

- 8. page 7,line 15: Once the optimal DIC parameters in terms of wake mixing have been evaluated using CFD, ... not sure CFD is used... - cf point 3 above? How did you determine optimal DIC parameters?

As explained in point 3, the CFD simulations were removed from the paper. The parameters chosen here are close to the optimum found in the wind tunnel.

- 9. page 8, line 9: please refer again to Turbsim, and IEC when you reference to NTM

  The references suggested by the referee have been added here.

- 10. Figure 8, check caption

  The erratum in the caption has been removed.

- 11. page 11, start of section 6.1: five different cases are mentioned, but later on, results of only three experiments seem to be reported (the ones with different amplitudes). What about results for block signal, and results for phase difference between turbines?

  The results of these last two experiments have been cut from the paper, since the results were as of yet inconclusive. However, the authors have overlooked this reference to these experiments, which was therefore not removed. This has been done now.

- 12. Figure 9: Im a bit confused: in the caption you mention different amplitudes, but in the legend (bottom-left panel) you seem to show averaged values for C_T (1, 1.5, 2). First of all are these averaged values of C_T (see table 2)? Therefore, do you mean different average & amplitude. Please clarify and improve caption/legend

  This figure shows, as mentioned in the caption, results for different amplitudes of excitation of C_T'. To remove any ambiguity, the legend has been changed to read Amplitude A instead of C_T. Furthermore, a reference to Table 2 is added, where the corresponding mean and amplitude of C_T and pitch angle β can be found.

- 13. page 15, line 4: It can therefore be concluded .... In the work of Munters, Sinusoidal DIC was shown to work for the first turbine, with a positive effect on the second, but not on the third. Sinusoidal DIC applied to the second (or later) turbines did not work. The results in the current paper seem to confirm this. Therefore, this conclusion should probably be adapted/tuned down a bit + maybe additional discussion on future work in the conclusions section.

  This comment is very similar to the first comment of Referee #1. For a more detailed response, the reader is therefore referred to the response given here. In short, the wind tunnel experiments show that the largest positive effect is measured at turbine 2, but there is also a (very small) positive effect at turbine 3. A more elaborate discussion on these results has been added to both Section 6.2 (results) and 7 (conclusions).

- 14. Continuing on the previous point: what about the results of the out-of-phase experiment with the first & second turbine (cf. comment 11 above) was this intended to improve turbine 3 performance if so, what were the results. Did you do in-phase as well? Reading the text, Im presuming that most experiments were only using sinusoidal DIC on the first turbine? Is that correct? Should maybe be emphasized/discussed a bit more throughout.

  First of all: yes, it is correct that in the results presented in this paper, periodic DIC was only applied on the first (upstream) turbine. To emphasize this, a mention of this is added once more both in Section 2 (Control Strategy) and Section 6 (Results).
  Secondly, regarding the experiments with periodic DIC on both turbines 1 and 2: as mentioned at the response to comment 11, these results were inconclusive. Based on the experiments, it could not be said whether this strategy would positively effect the power capture of the wind farm, nor what the influence of a phase offset was. Therefore, the choice was made not to include these results in this paper. This is possible future research direction though, and as such has been added to the conclusions.

- 15. page 15, line 15: to be fair, you should compare weighted DEL against weighted power gain (which will also be much lower when averaged over a Weibull distribution)

  The referee is absolutely right that the power gain weighted over a Weibull distribution would be significantly lower, as periodic DIC will only be effective when there is full wake interaction between turbines. However, this paper does not investigate the potential AEP of a wind farm. Rather, it shows that - when wake interaction is present - periodic DIC can be an effective method to increase power production, with the load effects being relatively small. As already mentioned in the conclusions, a future research challenge lies in further investigating the turbine loads with respect to the potential power gain.

- 16. page 16, line 1: significant differences between simulations and experiments. What do you mean by that? please clarify...

  There are some differences between the results found in simulations executed by Munters and Meyers, and the wind tunnel results presented in this paper. Most notably, the optimal frequency and amplitude of excitation is found to be slightly higher and lower respectively. To name these differences "significant" might be a bit too definite, so this was changed to "some minor differences". Furthermore, the aforementioned differences are now explicitly named in a prior paragraph of the conclusions.

Response to comments of Anonymous Referee #3

- The paper is well structured and makes a relevant contribution with first scaled wind tunnel experiments of dynamic induction farm control, as well as load evaluation by aeroelastic simulation for excited upstream wind turbine. Sound methodology is applied to results analysis. Publication is recommended upon addressing some minor comments listed below, added to those of the other referees.

  The authors would like to thank the referee for his constructive feedback in improving the quality of the paper.

- Page 8, Line 1: Which was the reason behind the choice of a pitch amplitude of 2 degrees? Could you please better specify? Has this pitch amplitude any relation to the amplitude used in the scaled tests?

  The pitch amplitude of 2 degrees leads, for the NREL 5MW turbine, to an excitation amplitude of C_T' of approximately $A = 1.5$. This case can therefore be considered an "average" load case. This clarification is now added to Table 1, where the different cases are defined.

- Besides, the experiments have shown greater dependency on the amplitude than on the frequency (Strouhal number). Wouldnt it be coherent to perform in future work the load simulations also in accordance to this by varying the pitch amplitude in order to see the effect on loading of changing such amplitude?

  The authors agree that this would be a very interesting future research direction. The analysis presented in this paper should really be seen as a first step in evaluating the load effects of DIC. Such an investigation would indeed be very interesting to perform. Further investigation into these loads has been added more explicitly to the future research possibilities in Section 7.

- Section 7- Conclusions could be further elaborated by gathering nice comments previously included in the paper and by precising better some aspects: It is shown that by acting on turbine 1, turbine 3 remains unaffected.

  The observation that "most of the gain [is] coming from the first downstream turbine" has been added to the conclusions.

- It is shown that, for a given mean wind speed, the change in the power gain mostly depends on the amplitude of the DIC and not on the frequency. Would it be any dependence on the mean wind speed? The experiments have examined the effect of DIC under different TI conditions. It would also be interesting to see in the future the effect under different mean wind speed conditions.

The authors absolutely agree with the referee that investigating the effect of different mean wind speed conditions would be very interesting. It would for example be very informative to check whether DIC would also work with above-rated wind speeds, when the pitch angle is already varied to ensure constant power output. Therefore, this suggestion has been added to the future research opportunities in Section 7.

- Page 15, Line 17 to Page 16, Line 1: In all, it can be concluded that the dynamic induction control approach shows great promise, as now both simulations and scaled experiments show that it is possible to achieve a power gain. However, significant differences are found between simulation and experiments, which still need to be addressed. The conclusion included does not apply to the presented simulation results, which consist in the simulation of one single turbine, mainly for loading evaluation. These simulations dont provide insights into the behavior and power gain at farm level. Equally, it is not clear which are the significant differences between simulation and experiments this statement makes reference to.

  This comment is similar to comment 16 of Prof. Meyers, so the response is also similar. This comment refers to differences between the results found in simulations executed by Munters and Meyers, and the wind tunnel results presented in this paper. This is now clarified more explicitly. Most notably, the optimal frequency and amplitude of excitation is found to be slightly higher and lower respectively. To name these differences "significant" might be a bit too definite, so this was changed to "some minor differences". Furthermore, the aforementioned differences are now explicitly named in a prior paragraph of the conclusions.

- Is there any hypothesis on why the increase in the DIC amplitude provokes such decrease in the final power gain?

  As already discussed in Section 6, the power loss is caused by a very significant drop in power production of the excited turbine with higher DIC amplitudes, for which downstream machines cannot fully compensate. A possible explanation for this could be a slight rotor imbalance which was present in the $G1$ models, which causes significant vibrations on the excited turbine for higher amplitudes of excitation. This explanation has been added to both Section 6 (results) and Section 7 (Conclusions).

- For practical application of the technology, taking into account that DIC is intended for region II -among others-, have you considered the possible risk of stall when applying a periodic pitch variation of several degrees around fine pitch? The value of 2 degrees used in simulations (section 5) could prove to be relevant.

Stall is not something we have looked into as of yet, although we are of course aware of this risk. However, this did not prove to be a problem in the scaled experiments, as quite extreme pitch variations (up to $\pm 5^{\circ}$) were used without stall issues. Investigating the risk of stall on full scale machines, although of course very interesting, is out of the scope of this research.

- The lowest tested amplitude for DIC has proved to be the best one. So, one question that arises is whether further decrease in the amplitude would lead to even better results. It would be interesting to determine in the future which is the minimum "A" that provides the maximum power gain.

  The authors fully agree with this observation. For this reason, it is also clearly mentioned in the conclusions that further experiments are necessary to determine the full possibilities of periodic DIC.

- In the wind tunnel experiments it has been possible to measure the thrust coefficient thanks to the knowledge about the wind conditions. This has allowed the determination by trial and error of the pitch variation in order to provide a thrust coefficient (amplitude, frequency) matching the desired one. How would this technology be applicable in real wind turbines where such detail of information about wind conditions is not so easily and precisely available?

  In the experiments presented here, a excitation of the collective pitch was used to create a certain desired thrust coefficient. Assuming the optimal settings are independent of the wind speed (which is yet to be investigated), the optimal pitch excitation could simply be used without knowledge on the wind conditions. However, a far more interesting solution, which is also mentioned in the future research opportunities, is to develop a closed-loop dynamic induction control algorithm, including an engineering model or observer to estimate the wind conditions. This controller would then determine the optimal DIC settings and would be able to adapt to changing wind conditions based on the latest measurements of, for example, the turbine power production.

- For the sake of clarity and reproducibility: It would be advisable to indicate upfront from the very beginning of the paper that it focuses on below rated conditions and excitation of collective pitch angle. Also, to leave an explanatory comment about induction as in-wake speed deficit.

  Both the below-rated testing conditions and the induction definition have been included in the introduction.

- Table 1: Missing frequency units in last row (Frequency of excitation in St). Its understood that it is Hz, but better to leave it explicit.

  As mentioned in the text, the Strouhal number St is actually dimensionless. For clarity, "[-]" was added after St to note this dimensionlessness.

- Table 2: Please make coherent the denomination for the amplitude variable A (third column in the table) with the description in the table caption (CT,DIC).

  Due to a different comment from another referee, the caption of Table 2 has been modified. The denominations are now all coherent.

- Page 7, Line 18: It could be added as examined load the hub torsional moment, taking into account that these results are presented in Table 3.

  The mention of the hub torsional moment has been added here.

- Page 8, Line 9: It could be added mean therefore indicating mean hub wind speed of

  The addition of the word "mean" has been implemented as requested.

- Figure 7 and Figure 8, caption: It could be added mean therefore indicating mean wind speed

  The addition of the word "mean" has been implemented as requested.

- Table 3. The table caption would be clearer if it is indicated that the percentages refer to improvement with respect to baseline. Equally, it is indicated AEP in the caption, although the values are not included in the table. The percentage of variation of power with respect to baseline is of great interest, in order to compare the order of magnitude with the results of turbine 1 in the wind tunnel experiments. So, it would be advisable to introduce such information, not only in terms of AEP, but also through a figure of comparison with baseline, for example power time plot corresponding to Figure 5.

  The caption has been augmented to include that the results are given with respect to the baseline. AEP values of the excited turbine have been included. To accomodate the desire of the referee, a figure of the AEP over time has also been added to the paper.

- Section 6. It would be advisable to indicate the layout of the wind farm tested in the wind tunnel, either through written explanation or through a descriptive figure.

  The authors completely agree that such a figure was missing from the paper. In Section 4, explaining the wind tunnel setup, the requested figure showing the layout of the wind farm in the wind tunnel has been added.

- Table 4, caption: Caption could be clearer by making reference to baseline: An overview of the total power increase with respect to baseline by applying

  As requested, the text "with respect to the baseline case" has been added in the caption of Table 4.

- Table 4 and Table 5: It would be advisable to indicate the frequency units (first row).

  The requested frequency units have been added as requested.

- Page 11, Line 5: When mentioning the change of +2% in blade root loads, it would be advisable to specify flapwise. Equally, when mentioning the negligible impact found in edge-wise and in the hub, it would be clearer to mention the respective percentages, since for edgewise, its only 0.4%, but for the hub it accounts for 1% to 2%.

  All suggested additions have been implemented.

- The discussion of load results is mainly done for St = 0.4 and St = 0.5, while the best fit for experiments is provided by St = 0.33 (low TI) and St = 0.29. Which would be the correspondence between the St results in the scaled tests and those for a full-scale model such as the one simulated in CP-LAMBDA?

  It is hard to say how the optimal Strouhal number scales with the turbine size. The full-sized turbines used by Munters and Meyers find an optimum of $St = 0.25$, and the Strouhal number does scale for rotor size, so it could be argued that the optimal Strouhal number is (relatively) independent on the rotor size. This is something that could still be investigated in the future. The analysis done here focusses on the possible load effects for different Strouhal numbers, without arguing which of these would be optimal for power production in this case. The discussion of the results has been changed to include $St = 0.3$.

- Page 11, Line 18: When making reference to the experiments with different amplitudes on a sinusoidal input, it would be convenient to introduce the reference to Table 2. Equally, it could be helpful to indicate again that the sinusoidal input is applied to the collective pitch, which is the range of variation of the pitch angle, and which correspondence this would have with the pitch angle in a full-scale wind turbine.

  The requested reference to Table 2 has been added. The authors feel that this refence suffices as all the information requested by the referee can be found in this table. By focussing on the amplitude of the C_T-excitation, the authors also feel that a notion on scalability of the pitch amplitude is unnecessary: this might differ per turbine, but can easily be calculated with the required C_T-β-tables.

- Page 13, Line 3. In the same way that it is indicated explicitly for low TI experiments (Page 11, Line 17), it would be nice to indicate the approximate value of TI applied in the high TI experiments.

  As requested, the high-TI value (10%) has been added here.

- Page 13, Line 6. For higher clarity, it could be indicated to which production it makes reference the sentence. It is understood that it refers to: the baseline power production of this turbine is already slightly lower than in low TI conditions.

  The referee is correct in his assumption. For clarity, the suggested addition has been made.

- Page 14, Line 8: For the sake of clarity, it would be advisable to introduce again the reference Schreiber et al. (2017), which was already indicated in Page 4.

  The requested reference has been added here.

- Page 3, line 8: were instead of where

  This erratum has been corrected.

- Table 1 The frequencies of excitation in St indicated for the aeroelastic simulations Between 0.3 and 0.5 dont match the range of frequencies of DIC stated in Section 5, Page 8, where it is stated that this frequency varies from 0.00952 Hz to 0.0595 Hz. Equally, the frequencies indicated for the experiments [0.09-0.41] dont match the frequencies included in Table 4 and Table 5 [0.5-2.3].

  The referee seems to confuse two different units here. In general, the frequency of excitation is expressed with the dimensionless Strouhal number, as defined in Section 2. This unit is also used in Table 1, so the values given here are dimensionless, not in Hertz. They do in fact match with the values of St given in Tables 4 and 5, as well as the values of St mentioned on page 8.
  To prevent such confusion in a future version of the manuscript, the word "frequency" has been removed from Table 1, which now reads "Strouhal number St of excitation [-]". Table 4 and 5 already contained both the frequency in Hertz as well as the Strouhal number, but units have been added to clarify the difference. Hopefully this removes the confusion and helps the referee understand the implemented control signals.

- Page 6, line 15: kHz instead of kH

  This erratum has been corrected.

- Figure 5, xlabel: It would be preferable to indicate time units in accordance to the symbol stated by the International System of Units: s

  The units have been changes from "sec" to "s".

- Figure 7 and Figure 8, xlabel: It could be introduced a space between Wind Speed and the unit [m/s]

  A space has been added before the unit.

- Page 11, Line 1: According to SI unit rules and style conventions, unit should not be italic m/s.

  The unit is no longer displayed in italic.

- Page 11, Line 3: In accordance to style convention, there should be a space between the number and unit 15 m/s

  A space has been added.

- Page 11, Line 22: It seems that the verb is missing in the sentence: the power is divided

  This is corrected as suggested by the referee.

- Figure 9, Caption: The reference in the figure legend and caption should be coherent between CT and CT.

  As a response to a different comment, the legend and caption of this figure has already been changed. The amplitude is now given by the variable A in both the legend and caption.

- Figure 11, legend: It seems that baseline would fit better than "benchmark", also keeping coherence with previous figures such as Figure 9.

  This has been corrected.

- Page 14, Line 2: It seems that the sentence However, since the power gain at turbine 3 is slightly lower, the total power is also lower than in the baseline case would indeed make reference to turbine 2, according to the figures.

  The referee is right in his assumption, and this has been corrected.

- Page 15, Line 15: To be corrected weighted instead of weighed.

  This has been corrected.

- It would be preferable to specify the increase of the weighted DEL with respect to baseline. Equally, the values of DEL included could be misleading without specifying which load they make reference to. Indeed, the 0.3-0.4% refers to blade root edgewise, which is the least affected by DIC.

  The addition "with respect to the baseline case" has been added, as well as the notion that these number refer to the blade root edgewise loads.

Response to comments of Anonymous Referee #4

- Dear authors, Thank you very much for submitting the paper to the WES journal. It was nice reading the paper and it is of high quality. Altogether a lot of relevant work is presented and it gives a significant contribution to the community. The paper follows a clear structure and gives a lot of background information that helps to understand the tasks that have been performed. Altogether I recommend the publication with the consideration of the following minor corrections and the comments of the other reviews.

  The authors would like to thank the referee for the compliments, as well as for the constructive feedback in improving the quality of the paper.

- Abstract: Please introduce the idea of induction control before naming it and extend the abstract a litte more. This would help people being not familiar with the topic to unterstand the content of the paper.

  The abstract has extended: it now includes a (very general) introduction into wind farm control as well as in induction control. The additions made are as follows: *As wind turbines in a wind farm interact with each other, a control problem arises that has been extensively studied in literature: how can we optimize the power production of a wind farm as a whole. A traditional approach is to this problem is called induction control, in which the induction factor, i.e. the in-wake wind speed deficit, of a turbine is lowered such that downstream turbines can increase their power capture.*

- Figure 1: Please explain the figure in more detail in the caption. This figure basically presents the whole concept and needs therefore more explanation.

  A much more elaborate caption has been added to this figure, to better explain the concepts shown here.

- p. 2 l.4: you say DTU 5 MW turbine: NREL 5 MW turbine

  This erratum has been corrected.

- Table 1: Munters et. al.

  This erratum has been corrected.

- Table 1: please first introduce beta and cT before having the table. I know that latex is placing it like this, but moving it to the next page is preferable.

  The paragraph introducing these variables is moved forward, such that it precedes the table, as well as the first mention of the table.

- Page 4: yaw control: to me wake steering is more familiar than yaw control. Maybe you need to add both or replace it

  Both "yaw control" and "wake redirection control" are now explicitly mentioned here.

- Figure 7-12: the style of the labels differ to the previous plots,

  The difference in style has been removed: all labels are now in "normal" letter style.

- Figure 7, 8: a space before unit (As mentioned in caption Fig. 8)

  The space before the units has been added.

- Conclusions: p.16 l.1: please again name the differences in the conclusions

  The differences, namely a slightly different optimal Strouhal number St and amplitude A, are now explicitly mentioned again in the conclusions.

- Acknowledgements: program: programme

  This erratum has been corrected.

Periodic dynamic induction control of wind farms: proving the potential in simulations and wind tunnel experiments

Joeri Frederik[a], Robin Weber[b], Stefano Cacciola[c], Filippo Campagnolo[b], Alessandro Croce[c], Carlo Bottasso[b], and Jan-Willem van Wingerden[a]

[a]Delft Center of Systems and Control, Faculty of Mechanical, Maritime and Materials Engineering (3mE), TU Delft. Mekelweg 2, Delft, The Netherlands
[b]Wind Energy Institute, Technische Universität München, Garching bei München, D-85748 Germany
[c]Dipartimento di Scienze e Tecnologie Aerospaziali, Politecnico di Milano, Milano, I-20156 Italy

Correspondence: Joeri Frederik (J.A.Frederik@TUDelft.nl)

Abstract. ~~In this paper,~~ As wind turbines in a wind farm interact with each other, a control problem arises that has been extensively studied in literature: how can we optimize the power production of a wind farm as a whole. A traditional approach to this problem is called induction control, in which the induction factor set-point, i.e., the ~~potential of Dynamic Induction Control (DIC), which has shown promising results in recent simulation studies, is further investigated.When this control strategy is implemented, a turbine varies its induction factor dynamically over time~~in-wake wind speed deficit, of a turbine is lowered such that downstream turbines can increase their power capture. In recent simulation studies, an alternative approach, where the induction factor is varied over time, has shown promising results. In this paper, ~~only periodic variation~~the potential of this Dynamic Induction Control (DIC) approach is further investigated. Only periodic variations, where the input is a sinusoid, are studied. A proof of concept for this periodic DIC approach will be given by execution of scaled wind tunnel experiments, showing for the first time that this approach can yield power gains in real-world wind farms. Furthermore, the effects on the Damage Equivalent Loads (DEL) of the turbine are evaluated in a simulation environment. These indicate that the increase in DEL on the excited turbine is limited.

1 Introduction

The interaction between wind turbines in a wind farm through their wake is a field of research as old as wind farms ~~itself~~themselves. The wake of ~~an upstream~~ a turbine has a wind field with a lower velocity and a higher Turbulence Intensity (TI), resulting in a lower power production and higher relative loads for downstream turbines. To exploit this interaction between turbines, induction control (sometimes called "derating"), with induction the in-wake speed deficit, has been a popular research topic in recent years. The concept of this control approach is schematically shown in Figure 1a. Despite initial promising results (Marden et al., 2013; Gebraad et al., 2013), recent studies indicate that the power gain that can be achieved with ~~this~~ steady-state ~~axial~~ induction control is limited to non-existing (Campagnolo et al., 2016a; Nilsson et al., 2015; Annoni et al., 2016).

~~Meanwhile, recent~~ An alternative approach, first mentioned in (Westergaard, 2013), is to actively manipulate wake recovery. Recent simulation studies (Goit and Meyers, 2015; Munters and Meyers, 2017) have shown that so-called Dynamic Induction

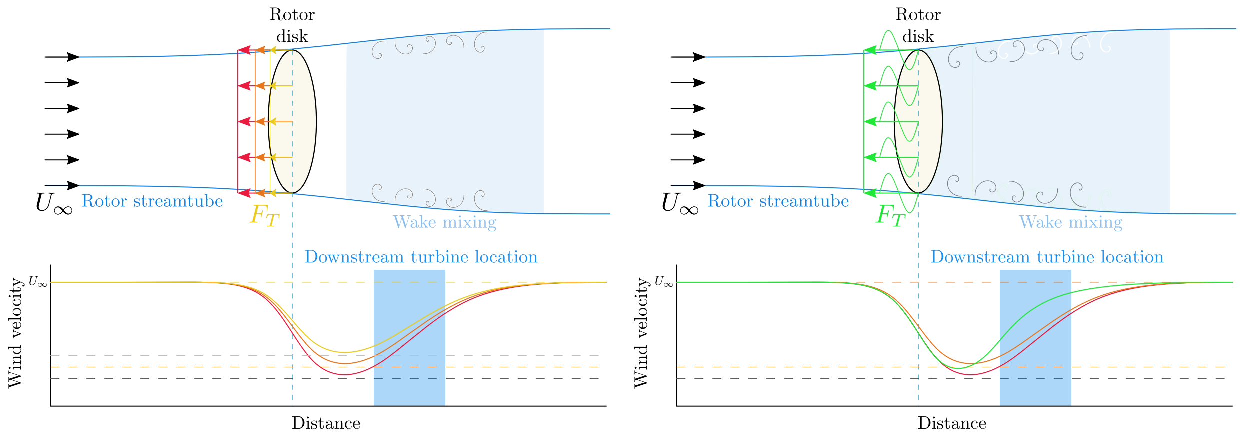

(a) Static induction control with different induction settings.

(b) Periodic dynamic induction control.

Figure 1. A schematic representation of a wind turbine in a flow field, showing the ~~streamtube~~ working principles of static (a) and dynamic induction control (b). On the top, the turbine is simplified as a rotor disk, and its streamtube - the area where the wind speed is affected by the turbine settings - is depicted. The force F_T exerted on the wind is shown for different ~~axial~~ induction settings, where red depicts greedy control, orange and yellow arbitrary static derating settings, and green periodic DIC. The bottom figures show the corresponding wind velocity ~~profile~~ profiles, with respect to inflow velocity U_∞ ~~is shown on the bottom~~, ~~with in blue~~ as a function of the distance from the turbine. The area ~~of interest~~ highlighted in blue is where a downstream turbine is typically located.

Control (DIC) improves the power production in small to medium-sized wind farms. This approach, where the induction factor is varied over time, ~~induces~~ generates a turbulent wind flow that enables enhanced wake recovery. Consequently, downstream turbines will compensate for the power loss of the upstream turbine, leading to a higher overall power production of the wind farm. The optimal dynamic control inputs are found using a computationally expensive adjoint-based Model Predictive Control (MPC) approach.

In Munters and Meyers (2018), a simpler approach is suggested: the induction variation is limited to a sinusoidal signal implemented on an actuator disk. This approach is here dubbed "periodic DIC". A grid search with different amplitudes and frequencies is performed to find the optimal dynamic signal in a high-fidelity simulation environment. The effect of this approach on the streamtube and downstream wind velocity is shown in Figure 1b. It should be noted that the applied excitation is very low-frequent. An optimal Strouhal number $St = 0.25$ is found, which corresponds to a period of approximately 56 seconds for ~~a DTU~~ an NREL 5 MW turbine (Jonkman et al., 2009).

However, no experiments have yet been executed that validate this approach on actual, either scaled or full-sized, wind turbines. Furthermore, the effects of DIC on the loads of the turbines are yet to be evaluated. This paper aims to bridge this knowledge gap by executing a thorough evaluation of DIC both in simulation environments and in wind tunnel experiments. The effects of DIC on the ~~wake of a turbine will be investigated. Simulations will be executed using the high-fidelity Computational Fluid Dynamics (CFD) environment SOWFA (Churchfield and Lee, 2012). The effects of DIC on the~~ loads on turbine level are evaluated using the aeroelastic tool Cp-Lambda (Bottasso and Croce, 2009–2018; Bottasso et al., 2006).

For the wind tunnel experiments, the Atmospheric Boundary Layer (ABL) wind tunnel of the Politecnico di Milano (Polimi) is used (Bottasso et al., 2014). Three `G1` models, which have a rotor diameter of 1.1 m and are developed by the Technical University of Munich (TUM) (Campagnolo et al., 2016a, b, c) will be used as turbine models.

To verify the validity of the periodic dynamic induction approach for fast wake recovery in a wind farm, a number of wind tunnel experiments in both low and high Turbulence Intensity (TI) conditions are executed. All experiments are executed at a below-rated wind speed, i.e., in operating region II. The effect of varying the amplitude and frequency of the signals is studied, and the performance of this approach is compared with other state-of-the-art wind farm control strategies. A positive result in these experiments would be an important step towards proving the validity of this approach in real wind farms.

The structure of this paper will be as follows: in Section 2, the DIC strategy will be explained. Sections 3 and 4 will elaborate on the simulation environment and the experimental setup, respectively. In Section 5, the simulation results will be presented, followed by the experimental results obtained in the wind tunnel in Section 6. Finally, the conclusions will be drawn in Section 7.

2 Control Strategy

In this section, the strategy behind dynamic induction control will be discussed shortly. As mentioned in the introduction, the approach presented in Munters and Meyers (2018) is used as a basis for this paper~~.~~: the thrust force of the upstream wind turbine is excited to induce wake mixing, in order for downstream turbines to increase their power capture. It is shown that the amplitude and frequency of a sinusoid determine the overall power production. The optimum found in here is a Strouhal number of $St = 0.25$, with an amplitude of the disk-based thrust coefficient $C_T' = 1.5$. The Strouhal number is defined as $St = fD/U_\infty$ for a given frequency f, rotor diameter D and inflow velocity U_∞, while $C_T' = 4a/(1-a)$, with a the axial induction factor (Goit and Meyers, 2015). This disk-based thrust coefficient relates to the thrust coefficient C_T as $C_T = C_T'(1-a)^2$. For the `G1` models and an inflow velocity of 5.65 m/s, this Strouhal number would result in an excitation frequency of approximately 1.3 Hz.

However, there are some fundamental differences between ~~this work~~ Munters and Meyers (2018) and the work presented here, which are summarized in Table 1. Due to the size of the wind tunnel (see Section 4), a 3-turbine wind farm is the deepest possible array configuration. The amplitude and frequency ranges ~~where~~ were slightly reduced due to time constraints. Finally, to allow for practical implementation on a turbine model, the collective pitch angle β of the upstream model was excited periodically. This results in a slightly different thrust signal, as shown in Figure 2, but simulations show that the difference in output for these input signals is limited.

Since the internal torque controller of the `G1` model is also active, the amplitudes and offsets of the pitch signals are tuned manually such that the resulting thrust coefficient matches the desired thrust coefficient in amplitude and frequency. To achieve this, the thrust force on the turbine is measured, which, together with knowledge about the wind conditions, is used to calculate the thrust coefficient over time.

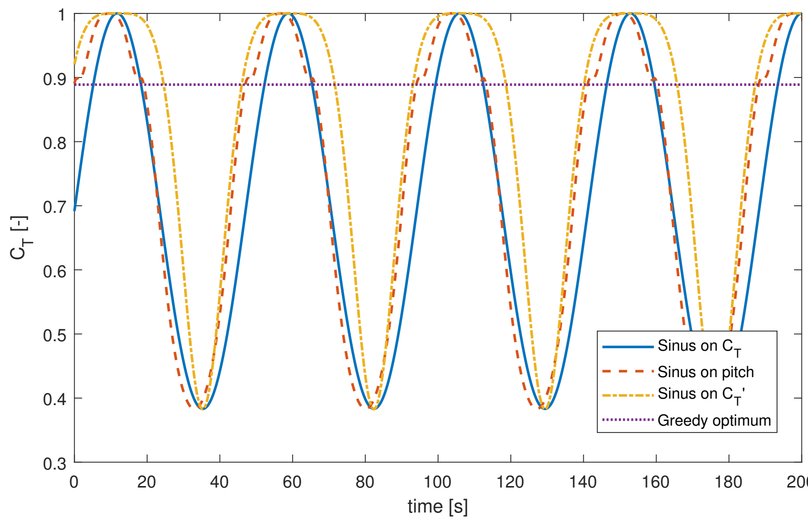

Figure 2. Values of C_T for different types of input signals, created using a ~~sine-like C_T' signal with amplitude $A = 1.5$, compared to a sine~~ look-up table of the `G1` turbine model. The thrust coefficient is shown for three different sinusoidal excitations: on C_T ~~resulting in a similar~~ , on C_T' and on the collective pitch angle β, tuned such that the amplitude of C_T' is 1.5. The dashed line shows the steady-state optimal C_T.

~~In Munters and Meyers (2018), it is shown that the amplitude and frequency of a sinusoid determine the overall power production. The optimum found in here is a Strouhal number of $St = 0.25$, with an amplitude of the disk-based thrust coefficient $C_T' = 1.5$. The Strouhal number is defined as $St = fD/U_\infty$ for a given frequency f, rotor diameter D and inflow velocity U_∞, while $C_T' = 4a/(1-a)$, with a the axial induction factor (Goit and Meyers, 2015). For the `G1` models and an inflow velocity of 5.65 m/s, this Strouhal number would result in an excitation frequency of approximately 1.3 Hz.~~

Finally, a comparison will be made with wind farm control approaches that have already been investigated more extensively in literature: static induction control (also called derating control) and ~~wake redirection~~ yaw control (also called ~~yaw~~ wake redirection control). The optimal control settings are found using the static `FLORIS` model ~~(Gebraad et al., 2016)~~

Table 1. Differences between the approach in Munters and Meyers (2018) and both the simulations and wind tunnel experiments presented in this paper. Note that the pitch amplitude $\beta = 2°$ used in the simulations leads to a amplitude of approximately $C_T' = 1.5$.

	Munters ~~e~~et. ~~a~~al.	**Simulations**	**Experiments**
Layout	4 turbines in a row	Single turbine	3 turbines in a row
Environment	LES code	Aero-elastic code	Wind tunnel experiments
Control input	Sinusoid on C_T'	Sinusoid on β	Sinusoid on β
Amplitude of excitation	C_T' of 0.5, 1, 1.5 and 2	$\beta = 2°$	C_T' of 1, 1.5 and 2
~~Frequency~~ Strouhal number St of excitation ~~in St~~[-]	Between 0.05 and 0.6	Between 0.3 and 0.5	Between 0.09 and 0.41

(Annoni et al., 2018). This parametric model is calibrated with wind tunnel measurements, as described in Schreiber et al. (2017). The control settings are then implemented on the same wind farm set-up in the wind tunnel such that a fair comparison can be made. In Section 6, the results of these experiments will be evaluated.

3 Simulation environment

In order to evaluate the effect of DIC on turbine level, the aeroelastic tool `Cp-Lambda` (Code for Performance, Loads, Aeroelasticity by Multi-Body Dynamics Analysis) (Bottasso and Croce, 2009–2018; Bottasso et al., 2006) has been used. This software is an aeroelastic code based on finite element multibody formulation, which implements a geometrically exact non-linear beam formulation (Bauchau, 2011) to model flexible ~~element~~ elements such as blade, tower, shaft and drive train. The generator-drive train model can include speed-dependent mechanical losses. The rotor aerodynamics are modelled via blade element momentum (BEM) theory or a dynamic inflow model, and may consider corrections related to hub- and tip-losses, tower shadow, unsteadiness and dynamic stall, whereas lifting lines can be attached to both tower and nacelle to model the related aerodynamic loads.

For the fatigue analysis, the model of the NREL 5 MW reference wind turbine (Jonkman et al., 2009) was considered. This reference 5 MW wind turbine has a rotor diameter of 126 m and a rated wind speed of 11.4 m/s. ~~A region I-1/2 with constant rotor speed equal to 6 rpm extends from the cut-in speed of 4 m/s to 7 m/s.~~ Each blade is discretized with 30 cubic finite elements, the tower with 20 cubic elements. Additionally, pitch and torque actuators are modeled respectively as second and first order systems and the model is completed by a standard PID controller (Jonkman et al., 2009). Finally, 10-minute wind time histories of turbulence class “A”, according to DLC 1.1 of IEC 61400-1 Ed.3. (2004), generated by the software `TurbSim` (Jonkman and Buhl, 2006), were given as input to the aeroelastic solver.

4 Experimental Setup

The experimental results presented in this paper were gathered by performing dedicated tests within the wind tunnel of the Politecnico di Milano (Polimi), which is a closed-return configuration facility arranged in a vertical layout and equipped with two test rooms. A detailed description of the facility can be found in (Bottasso et al., 2014). The tests were performed within the boundary layer test section, which has been conceived for civil, environmental and wind energy applications. This section has a large cross-sectional area of 13.84×3.84 m, which allows for low blockage effects even with several relatively large turbine models installed within the test section.

Roughness elements located on the floor and turbulence generators placed at the chamber inlet are commonly used to mimic to scale the atmospheric boundary layer in terms of vertical shear and turbulence spectrum. During the experiments described later on, two boundary layer configurations were used: one generating low turbulent (~~Low-TI~~low-TI) and one generating highly turbulent (~~High-TI~~high-TI) flow conditions. These conditions roughly correspond to off- and onshore operation respectively. The flow characteristics are shown in Figure 3 together with the extension of the model’s rotor disk along the vertical axis. The coefficients of the vertical-shear exponential law, shown in the same picture, that best fit the experimental data are 0.144 and 0.214 for the Low-TI and High-TI cases respectively.

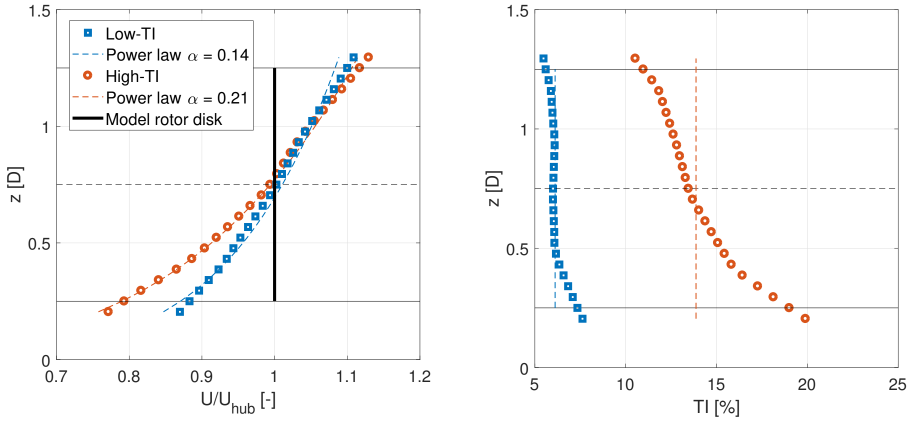

Figure 3. Vertical wind speed profile (a) and turbulence intensity (b) as a function of height above the tunnel floor, for low (low-TI) and high (High-TI) turbulence experiments.

4.1 Wind turbine models

~~Up to three~~ Three `G1` wind turbine models developed at TUM were used to perform the experiments reported in this paper. This model type was widely employed and described in detail in previous research (Campagnolo et al., 2016a, b, c) and is shown within the boundary layer test section of the Polimi wind tunnel in Figure 4. The setup of the turbines in the tunnel is shown in Figure 5.

With a rotor diameter of ~~1.1~~ $D = 1.1$ m and a rated rotor speed of 850 rpm, the model was designed to have a realistic energy conversion process and wake behavior: it exhibits a power coefficient $C_\mathrm{P} \approx 0.41$ and a thrust coefficient $C_\mathrm{T} \approx 0.81$ for a tip speed ratio $\lambda \approx 8.2$ and a blade pitch $\beta \approx 0.4°$.

The turbine is actively controlled with individual pitch, torque and yaw actuators and features comprehensive on-board sensorization. Three individual pitch actuators and connected positioning controllers allow for an overall accuracy of the pitch system of 0.1 degrees for each blade and the ability to oscillate the blade pitch with an amplitude of 5 degrees at 15 Hz around any desired pitch angle. Strain gauges are installed on the shaft to measure bending and aerodynamic torsional loads, as well as at the tower foot to measure fore-aft and side-side bending moments. A pitot tube, placed three rotor diameters upstream of the first turbine model, provides measurements of the undisturbed wind speed at hub height. Finally, air pressure, temperature and humidity transducers allow for measurements of the air density within the test section. The measurements of these sensors are used to determine the performance of the turbine models. The thrust coefficient is obtained using measurements of the pitot tube wind speed measurement and fore-aft bending moment, while correcting for the effects of the tower and nacelle drag.

Figure 4. A G1 scaled wind turbine model within the wind tunnel of the Politecnico di Milano. The yellow and red arrows show the pitch and yaw control possibilities respectively. The yellow spires and bricks in front of the model create the high-TI flow conditions.

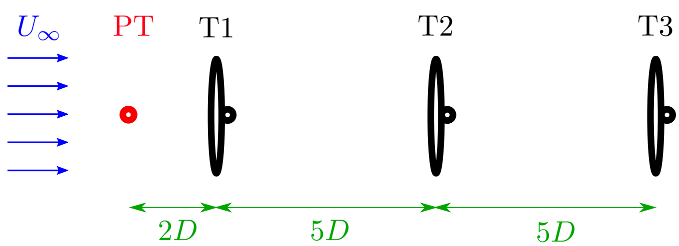

Figure 5. A ~~G1 scaled~~ schematic top view of the wind ~~turbine model within~~ farm setup in the wind tunnel~~of the Politecnico di Milano~~. The ~~yellow and red arrows show~~ pitot tube (PT), which measures the ~~pitch and yaw control possibilities respectively. The yellow spires and bricks~~ inflow velocity, is located 2 rotor diameters D in front of Turbine 1 (T1). The spacing between the ~~model create~~ turbines is $5D$ and the ~~high-TI flow conditions~~wind flows from left to right.

4.2 Control system

For each wind turbine model, control algorithms are implemented on a real-time modular Bachmann M1 system. Demanded values (e.g. pitch angle or yaw angle references) are then sent to the actuators, where the low level control is performed. Torque signals, shaft bending moments and rotor azimuth position are recorded with a sampling rate of 2.5 ~~kH~~kHz, while all other measurements are acquired with a sampling rate of 250 Hz. A standard power controller is implemented on each M1 system based on Bossanyi (2000), with two distinct control regions. Below rated wind speed, blade pitch angles are kept constant, while the generator torque reference follows a function of the rotor speed with the goal of maximizing the energy extraction. Above rated wind speed, the generator torque is kept constant and a proportional-integral (PI) controller adjusts the

Table 2. Average $\bar{C}_T$ and amplitude ~~$C_{T,\mathrm{DIC}}$~~ A_{C_T} of the three different thrust coefficient oscillations whose results are discussed in Section 6, as well as the mean pitch angle average $\bar{\beta}$ and amplitude A_β used to achieve these signals. Note that, as explained in Section 2, these collective pitch settings are not identical for different frequencies. Instead, they are tuned such that the mean and amplitude of C_T as given below are followed as accurately as possible.

Amplitude C_T'	$\bar{C}_T$ [-]	~~A~~ A_{C_T} [-]	$\bar{\beta}$ [deg]	A_β [deg]
~~$C_T' = 1$~~ $A = 1$	0.8	0.17	0.7	1.7
~~$C_T' = 1.5$~~ $A = 1.5$	0.7	0.3	1.8	2.8
~~$C_T' = 2$~~ $A = 2$	0.5	0.5	4	5

collective pitch of the blades in order to keep the generated power at the desired level. All experiments presented in this work are performed below rated wind speed.

For the tests performed within the research described in this paper, the standard power controller was augmented in order to enable the rotor thrust coefficients following a specific sine wave function. However, there is not a unique way of achieving this goal, since a specific thrust coefficient $C_T(\lambda, \beta)$ can be obtained by operating at different combinations of tip-speed-ratio λ and blade pitch β. In turn, the tip speed ratio can be varied either by changing the reference followed by the generator torque or changing the blade pitch. In this paper, a strategy that only changes the blade collective pitch is adopted. The implementation of this strategy simply requires changing the collective fine pitch at which the model blades are set when the machine operates in partial load conditions (region II). The fine pitch was tuned experimentally, by means of a trial and error procedure conducted with a stand-alone model, to achieving the desired mean $\bar{C}_T$ and amplitude A as reported in Table 2. The effects of these control actions in terms of impacts on the power output of the 3-turbine wind farm will be discussed in Section 6.

5 Simulation Results

~~Once the optimal DIC parameters in terms of wake mixing have been evaluated using CFD~~To evaluate the effects of DIC on the loads of the excited turbine, a full set of aeroelastic turbulent simulations (DLC 1.1) has been executed. These analyses have been conducted on the NREL 5 MW wind turbine with the main goal of quantifying the effect of this DIC on the fatigue loads. The analysis focuses mainly on the main wind turbine sub-components, such as the blade root flap- and edge-wise loads, as well as the tower base fore-aft bending and hub torsional moments.

~~The~~ DIC was assumed to be activated for wind speeds between 3 and ~~15~~ 25 m/s, to cover the totality of regions I-1/2, II, II-1/2 and ~~the first part of region~~ III. Notice that ~~15~~25 m/s seems a rather high speed, considering the fact that ~~in the full power region DIC might not be necessary~~so far, the effectiveness of DIC has only been evaluated in region II. In region III, the lower rotor inductions (i.e a lower in-wake speed deficit) may guarantee, together with the high inflow velocity, the full power region for the downwind rotor(s). Nevertheless, in the 10-minute simulation, the high turbulence intensity (class "A") causes a relatively long period where the mean wind speed is below the rated one and hence ~~the~~ DIC may have an important effect on

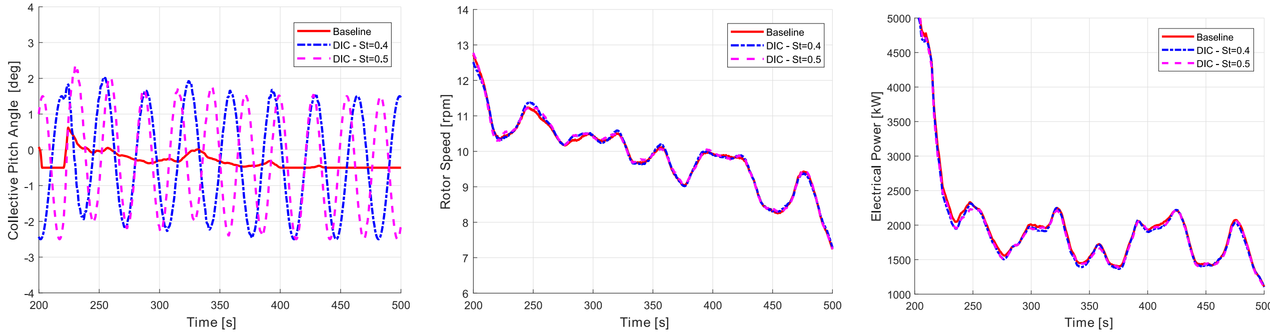

Figure 6. Comparison of pitch activity (left)~~and~~ , rotor speed (middel) and power (right) between baseline (solid red) and DIC controlled with $St = 0.4$ (dash-dotted blue) and $St = 0.5$ (dashed magenta) turbine for NTM class "A" at 9 m/s.

the wake. From this point of view, extending the authority of DIC up to ~~15~~25 m/s is to be regarded as a conservative choice. For clarity, the rated wind speed of 11.4 m/s will be shown in the figures showing the DELs at different mean wind speeds.

~~A Strouhal number of $St = [0.3 - 0.5]$~~ Strouhal numbers of $St = [0.3, 0.4, 0.5]$ and a pitch amplitude $\beta_{\mathrm{DIC}} = 2°$ were used in the aeroelastic simulations of the 5 MW turbine. Considering the diameter of this wind turbine model (126 m), the frequency of DIC f_{DIC} is between ~~9.52~~6.94$\cdot 10^{-3}$ Hz at 3 m/s (and $St = 0.4$) and 5.95$\cdot 10^{-2}$ Hz at 15 m/s (and $St = 0.5$), which correspond to a period equal to between 105 and 16.8 s respectively.

Due to the relatively low excitation frequency, the baseline turbine control is able to trim the machine without a significant additional effort or detrimental performance. Moreover, a coalescence between the DIC input frequency and turbine vibratory modes is not to be expected, at least for on-shore or off-shore turbines installed on rigid foundations.

Figure 6 shows an example of the time response of the machine with and without ~~the~~ DIC. These simulations have been performed with a Normal Turbulence Model (NTM) of class-A wind ~~with a~~ (IEC 61400-1 Ed.3., 2004) with a mean hub wind speed of 9 m/s, ~~a condition where~~ generated with `TurbSim` (Jonkman and Buhl, 2006). In these conditions, the wind turbine baseline control switches between region II, II-1/2 and III. ~~This~~ The figure shows the baseline condition, i.e., the one without the DIC controller, and two simulations with Strouhal number $St = 0.4$ and $St = 0.5$. The plot on the left refers to the pitch activity, ~~whereas the plot on the right~~ the plot in the middle to the rotor speed and the plot on the right to the power. The collective pitch angle time histories show the DIC activity superimposed to the trim-pitch. As can be seen, the rotor speed and power production with DIC active ~~behaves~~ behave very similar to that of the baseline case (solid lines), showing that the addition of the periodic pitch motion is not detrimental in terms of trimmer performance.

Figure 7 shows the power spectral density (PSD) of the rotor speed (left) and blade root flapwise bending moment with a NTM at 15 m/s, again for the baseline case (solid-red) and for DIC with Strouhal numbers $St = 0.4$ and $St = 0.5$. Both figures show a new frequency corresponding to the DIC excitation. This peak is far from the other aeroelastic frequencies of the wind turbine (the first being the tower fore-aft at $f = 0.31 Hz$), but may have an important role on the fatigue loads.

From the 10-minute simulations computed according to DLC 1.1 of IEC 61400-1 Ed.3. (2004), the stochastic time histories of the wind turbine loads are converted into simplified Damage Equivalent Loads (DELs) through a rainflow analysis and

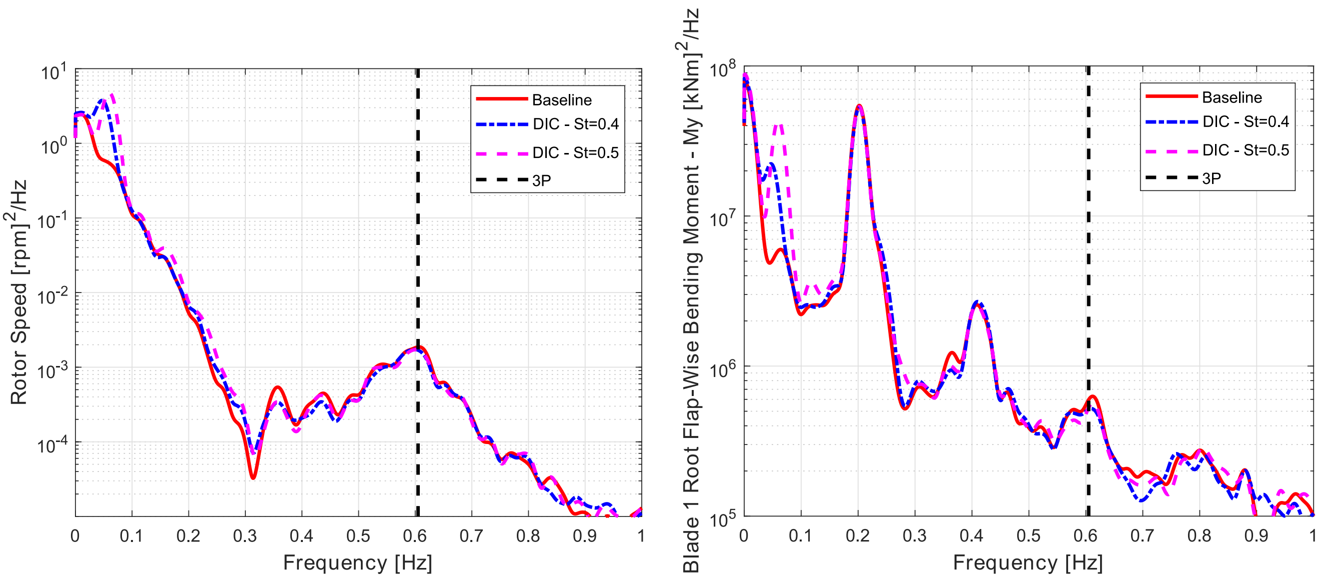

Figure 7. PSD comparison of the rotor speed (left) and blade root flap-wise bending moment (right) between baseline (solid red) and DIC controlled with $St = 0.4$ (dash-dotted blue) and $St = 0.5$ (dashed magenta) turbine for NTM class "A" at 15 m/s.

depicted in Figures 8 and 9 as a function of the mean wind speed. These figures show that DELs computed for the baseline case are almost always lower compared to when DIC is active, as would be expected based on Figure 7. For each mean wind speed, the DIC frequencies correspond to Strouhal numbers 0.4 and 0.5. Even though DIC is only effective at lower wind speeds, it is assumed active in the entire region III. As can be seen, the tower base fore-aft bending moment and the blade root flapwise are affected the most by this controller. As expected, the blade edge-wise bending moment is only slightly affected, since the DEL in edge-wise direction is mainly driven by gravity.

In order to have a more comprehensive indication about the impact of DIC on fatigue loads, one can consider the Weibull-weighted DELs, i.e., the DELs weighted throughout the probability distribution of the wind as expressed by the Weibull distribution $p_w(V)$

$$p_w(V) = k\frac{V^{(k-1)}}{C^k}\mathrm{e}^{-\left(\frac{V}{C}\right)^k}, \tag{1}$$

where k is the shape parameter and $C = 2V_{\mathrm{av}}/\sqrt{\pi}$ the scale factor and V_{av} the average wind speed.

The Weibull-weighted DEL, DEL_w, is hence computed as

$$\mathrm{DEL}_w = \int_{V_{\mathrm{CI}}}^{V_{\mathrm{CO}}} p_w(V)\,\mathrm{DEL}\,\mathrm{d}V, \tag{2}$$

where V_{CI} and V_{C0} are respectively the cut-in and cut-out wind speed.

Considering the class "A", where the Weibull distribution has $k = 2$ and ~~$V_{av} = 10\ m/s$~~$V_{\mathrm{av}} = 10$ m/s, it is possible to compute the Weibull-weighted DEL for the previously considered loads. To this aim, we suppose to switch off the DIC controller

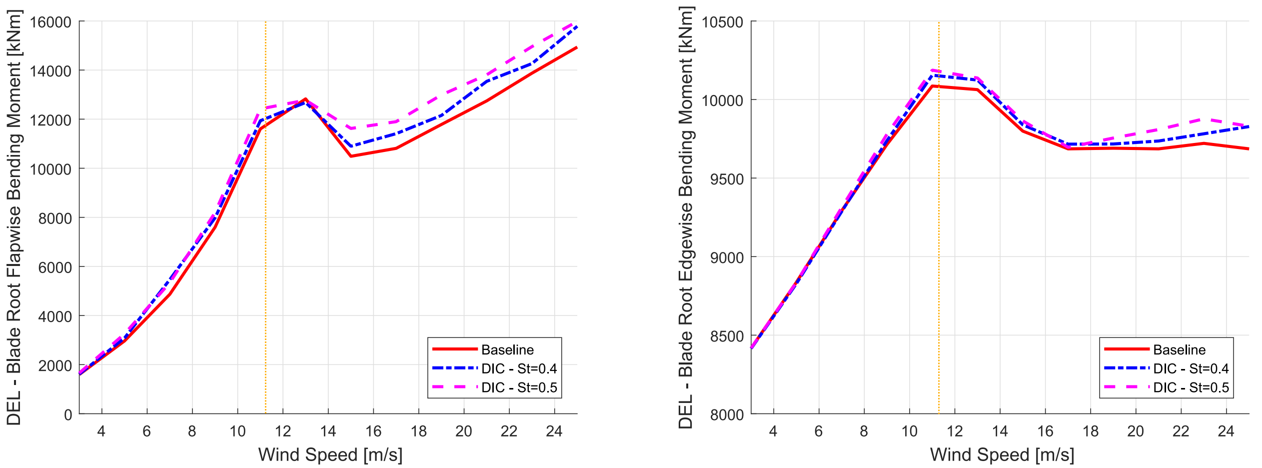

Figure 8. Comparison between blade root flap-wise (left) and edge-wise (right) DEL of the baseline (solid red) and DIC with $St = 0.4$ (dash-dotted blue) and $St = 0.5$ (dashed magenta) as functions of mean wind speed. The dashed yellow line indicates the rated wind velocity. Typically, DIC will only be implemented at below-rated inflow velocities.

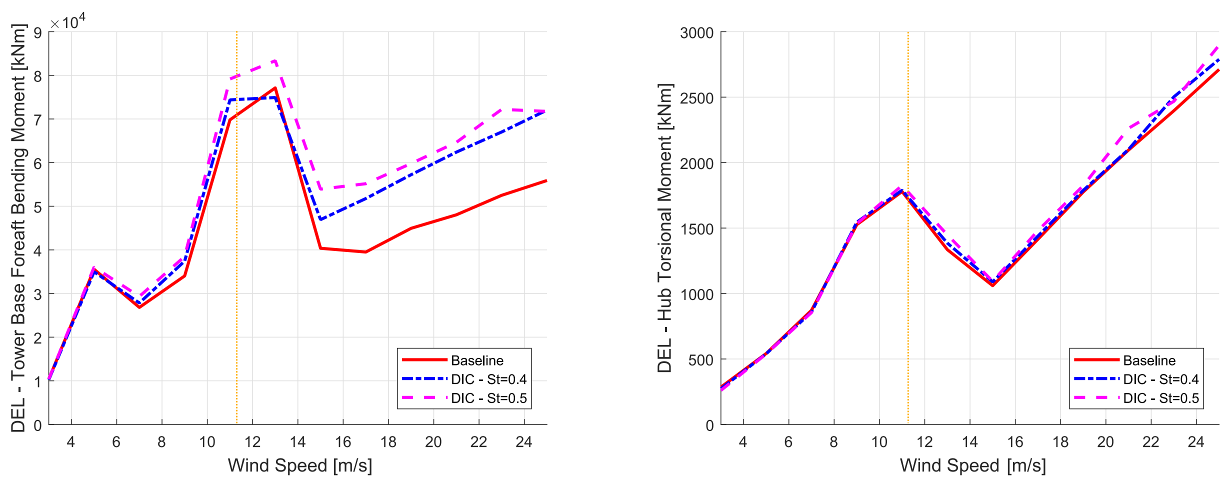

Figure 9. Comparison between tower base fore-aft bending moment (left) and hub torsional moment (right) DEL of the baseline (solid red) and DIC with $St = 0.4$ (dash-dotted blue) and $St = 0.5$ (dashed magenta) as functions of mean wind speed. ~~Space before unit in xlabel~~The dashed yellow line indicates the rated wind velocity. Typically, DIC will only be implemented at below-rated inflow velocities.

Table 3. Percentage increases of the Weibull-weighted DEL and AEP of the excited turbine compared to the baseline for different Strouhal numbers

	Blade Edgewise	Blade Flapwise	Tower ForeAft	Hub Torsion	AEP
$St = 0.3$	+~~0.41~~0.21%	+~~4.92~~2.66%	+ ~~11.78~~7.06%	+~~1.80%~~ 0.94%	-0.46%
$St = 0.4$	+0.40%	+1.80%	+ 7.26%	+1.67%	-0.54%
$St = 0.5$	+~~0.21~~0.41%	+~~2.66~~4.92%	+~~7.06~~11.78%	+~~0.94%~~ 1.80%	-0.59%

at wind speeds higher than ~~15m~~15 m/s, so that in region III the DELs are lower than the ones shown in the previous figures and equal to the baseline values. These results are summarized in Table 3. As can be seen, the tower base load is affected the most (~~about 7%~~7 to 11%), while loads on the blade ~~root~~ flapwise root loads increase with about 2%. A negligible impact (+0.4%) is found in the blade edge-wise and in the hub (1 to 2%).

~~Up to now~~So far, the analysis has not considered the probability of activation of the DIC-based wind farm control, which will depend on the specific farm layout and wind rose. From this point of view, the computed DEL increments seen before, as well as the AEP decrease, are to be considered as the ~~maximum possible obtainable~~worst possible case, as if DIC would always be implemented regardless of wind direction and subsequent wake interaction. It is therefore possible to assess that the impact of DIC on turbine fatigue loads for the analyzed NREL 5 MW reference machine is small compared to the possible gains.

6 Experimental Results

In this section, the results of the experiments executed in the wind tunnel at Polimi, as described in Section 4, will be presented. The effects of periodic DIC on the power production of a 3-turbine wind farm are presented for two cases, similar to onshore and offshore wind conditions. The performance of DIC will be compared with the state-of-the-art wind farm control strategies: greedy control, "static" induction control and wake redirection control.

6.1 Power production

First, the results with low turbulent wind (TI of approximately 5%) are evaluated. For this case, ~~5~~ 3 different sets of experiments have been conducted~~: three experiments with different amplitudes on a sinusoidal input, one with a block signal on the input and one where a sinusoid is put on both the first and the second turbine. In this last experiment, the phase difference between the two turbines is varied~~, as defined in Table 2. These sets each represent one specific amplitude of excitation of the upstream machine: an amplitude of $A = 1, 1.5$ and 2 of C_T' respectively. All other machines operate at their greedy optimum.

Figure 10 shows the mean power of the turbines and the total wind farm. To account for the small variations in flow conditions, the power is divided by the available power in the wind. As such, these values can be seen as power coefficients. Increasing the amplitude of the sinus decreases the power coefficient of turbine 1, while it increases the power coefficient of

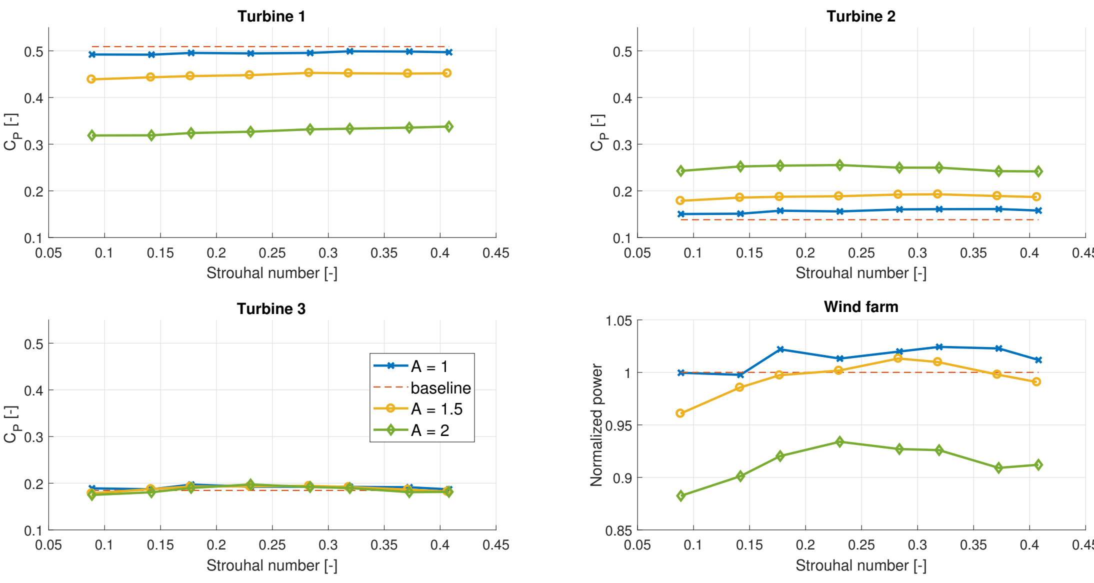

Figure 10. $\bar{C}_P$ of the wind farm in low TI conditions for different amplitudes A of C_T', as defined in Table 2. The bottom right figure shows the total power conversion compared to the baseline case.

~~turbine 2.~~ the downstream machines. However, for higher ~~C_T'~~ A, the loss at turbine 1 is too significant to compensate for by the downstream turbines. The unexpectedly high power loss at turbine 1 could partly be caused by a rotor imbalance that is worsened by higher amplitudes of excitation, leading to significant vibrations of the excited machine. As a result, the case with the lowest amplitude proves to be the most effective.

The highest increase in power extraction is found with ~~$C_T' = 1$ and $St = 0.33$~~ $A = 1$ and $St = 0.32$, resulting in a 2.4% gain. It should be noted that this gain is mostly obtained at turbine 2, while the power at turbine 3 is only marginally higher than in the baseline case. This corresponds to the conclusions drawn in Munters and Meyers (2018), where a positive effect is observed for turbine 2, but not for machines further downstream. Table 4 gives an overview of the effect of different amplitudes and frequencies on the power production of the 3-turbine model wind farm.

For the sake of reproducibility, Figure 11 shows the measurements of thrust coefficients C_T and C_T', as well as the pitch signal and rotor speed during 10 s of experiments in the optimal control settings ($St = 0.32$, $A = 1$). It should be noted that the thrust coefficient is obtained by using the definition

$$C_T = \frac{F_T}{0.5 \rho A_r U_\infty^2}, \tag{3}$$

where F_T is the thrust exerted on the rotor by the wind, ρ the air density, A_r the rotor area and U_∞ the inflow wind velocity. F_T is determined using the fore-aft bending moment, compensating for tower and nacelle drag, and the pitot measurements in front of turbine 1 (see Figure 5) are used as data for U_∞. This results in a C_T-signal disturbed by high frequency noise.

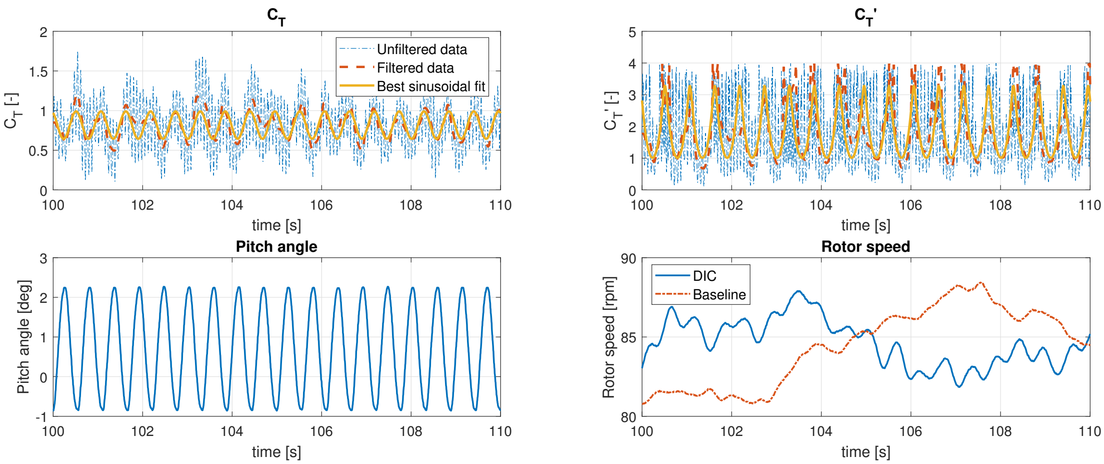

Figure 11. Clockwise, the measured C_T, C'_T, rotor speed and pitch angles of turbine 1 are shown during 10 s of the optimal $St = 0.32$, $A = 1$ DIC experiments in low TI. In the first two figures, the unfiltered data, low-pass filtered data and a best sinusoidal fit are shown. In the fourth figure, the rotor speed during 10 s of the baseline experiment is shown for comparison.

For this purpose, a low-pass filter with a passband frequency of 12.5 Hz was designed. This filter removes the high frequent noise signals, while keeping the excitations caused by DIC (at $f \leq 2.3$ Hz) intact. Furthermore, a sinusoid is fitted on the measurement data using the MATLAB-function LSQCURVEFIT. This function determines the amplitude, offset and phase of the sinusoid that best fit the data. The original data, filtered data and fitted sinusoid are all shown in Figure 11. Finally, the pitch excitation and rotor speed are depicted, the latter clearly showing oscillations caused by DIC. However, these oscillations are relatively small compared to variations caused by changing wind conditions, as the baseline rotor speed shows.

Table 4. An overview of the total power increase with respect to the baseline case by applying dynamic induction control with different amplitudes (A, rows) and frequencies (columns) for the low TI case.

Frequency [Hz]	0.5	0.8	1	1.3	1.6	1.8	2.1	2.3
Strouhal~~no.~~ [-]	0.09	~~0.15~~ 0.14	0.18	~~0.24~~ 0.23	~~0.29~~ 0.28	~~0.33~~ 0.32	~~0.38~~ 0.37	~~0.42~~ 0.41
A = 1.0	-0.04%	-0.24%	+2.20%	+1.30%	+1.6%	**+2.4**%	+2.3%	+1.2%
A = 1.5	-3.92%	-1.44%	-0.27%	+0.20%	**+1.3**%	+1.0%	-0.20%	-0.92%
A = 2.0	-11.76%	-9.89%	-7.97%	**-6.61**%	-7.30%	-7.41%	-9.09%	-8.80%

Finally, the reliability of these results will be examined. To do this, the results are divided into four segments of 60 seconds. These shorter segments of measurements, still containing 15000 measurement points and between 30 (0.5 Hz) and 138 (2.3 Hz) sine cycles, will then be used to determine the variance of the measurements.

Figure 12 shows box plots of these data sets for $A = 1$, normalized by the steady state optimal C_P of turbine 1. This figure shows that the variance becomes larger at each downstream row due to the increased turbulence. As a result, the variance is

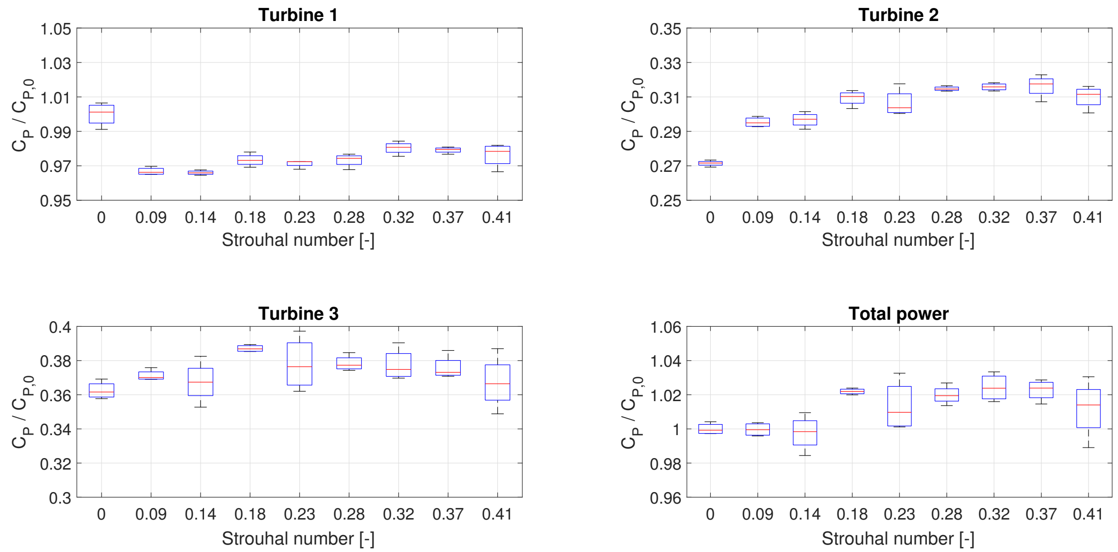

Figure 12. A boxplot showing the variance of the C_P measurements for the low turbulent, $C_T' = 1$ experiments, for all turbines individually as well as for the entire wind farm. The $f = 0$ measurement represents the baseline case of no dynamic control.

significant in the total power production: up to $\pm 2\%$ of the power. However, this figure also shows that the variance is lower than the power gained by using dynamic induction control: the lowest values of the box plot around the optimal frequency of 1.8 Hz are still higher than the baseline value. This analysis therefore indicates that the power increase is significant, as it is not a coincidental result of measurement errors.

Table 5. An overview of the total power increase by applying dynamic induction control with different amplitudes (A, rows) and frequencies (columns) for the high TI case.

Frequency [Hz]	0.5	0.8	1	1.3	1.6	1.8	2.1	2.3
Strouhal~~no.~~ [-]	0.09	~~0.15~~ 0.14	0.18	~~0.24~~ 0.23	~~0.29~~ 0.28	~~0.33~~ 0.32	~~0.38~~ 0.37	~~0.42~~ 0.41
$A = 1.0$	+1.4%	+1.5%	+2.4%	+1.4%	**+4.0**%	+1.8%	+0.8%	+2.3%
$A = 1.5$	-3.1%	-1.8%	-0.9%	**-0.8**%	-1.0%	-2.3%	-3.4%	-3.6%
$A = 2.0$	-8.9%	-8.7%	-5.2%	-6.7%	-7.7%	**-6.3**%	-8.0%	-8.1%

~~The same experiments were conducted in~~ Next, the results of the experiments with high turbulence intensity conditions (TI of approximately 10%) will be shown. The results ~~of~~ for all the amplitudes and frequencies that were studied are shown in Figure 13. The main conclusion that can be drawn from this figure, is that the effect of exciting the first turbine on the power production of this turbine is lower in these conditions. Due to the turbulence, the baseline power production of this turbine is already slightly lower than in low TI conditions. As a result, the power loss at turbine 1 is negligible for the $A = 1$ case. As the power gain at the downstream turbines is similar, the total power gain for this case is 4 %. This gain is found with $A = 1$ and $\cancel{St = 0.29}$$St = 0.28$, as can be seen in Table 5 where the results are summarized.

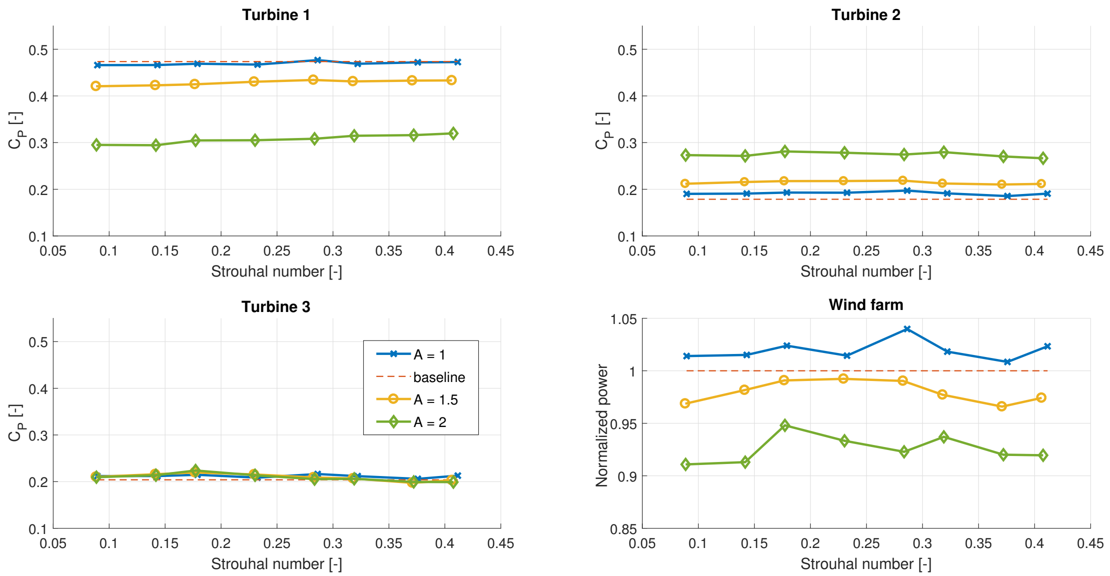

Figure 13. $\bar{C}_P$ of the wind farm for different amplitudes A of C_T', as defined in Table 2, in the high TI case. The bottom right figure shows the total power conversion compared to the baseline case.

When the amplitude of the excitation is increased, the power loss at turbine 1 is comparable with the results in low TI conditions. However, since the power gain at turbine ~~3~~ 2 is slightly lower, the total power is also lower than in the baseline case. Subsequently, it seems that the amplitude of the excitation is more important than the frequency in these conditions.

6.2 Controller comparison

To emphasize the value of the results shown in the previous subsection, a comparison of the effectiveness of the periodic DIC approach with state-of-the-art wind farm control approaches is executed in the case of full wake interaction. The optimal inputs are found using the steady-state FLORIS model ~~(Gebraad et al., 2016)~~(Annoni et al., 2018; Doekemeijer and Storm, 2018), which is calibrated using measurements from the wind tunnel (Schreiber et al., 2017). Three different control strategies are investigated:

- *Greedy control*: all turbines operate at their individual optimum, disregarding wake interaction between turbines~~due to their wakes~~.

- *Static induction control*: the induction settings (i.e.~~–~~, collective pitch angles) that predict the highest power capture according to the calibrated FLORIS model are implemented.

– *Yaw control*: the yaw angles that predict the highest power capture according to the calibrated `FLORIS` model are implemented.

The results of these experiments are shown in Figure 14. Similar to results in literature (Campagnolo et al., 2016a), static induction control is found to be unable to increase the power production of this wind farm. Yaw control on the other hand results in a benefit of 3.1 % As reported earlier, DIC was able to increase the power production with 2.4 % in these conditions. It can therefore be concluded that the potential profit of periodic DIC is significantly higher than with static induction, while it is comparable to that of yaw control when full wake interaction is present.

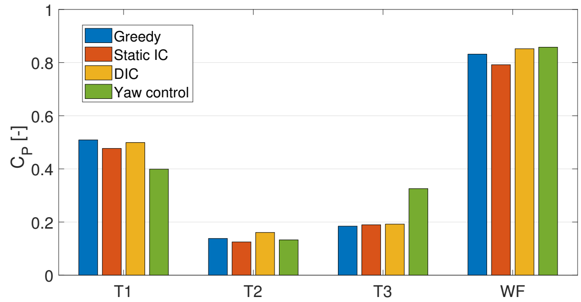

Figure 14. The power capture of three state-of-the-art control approaches compared with periodic DIC in low TI conditions. The power capture of the three individual turbines (T1-3), as well the total wind farm (WF) is shown.

7 Conclusions

In this paper, the effect of periodic Dynamic Induction Control (DIC) on both individual wind turbines and on small wind farms is investigated. For this purpose, both ~~high-fidelity~~ aero-elastic simulation tools and scaled wind tunnel experiments are ~~executed~~used. The unique wind tunnel experiments with DIC show, for the first time, that this control approach not only works in a simulation environment, but also in real world experiments. The results strengthen the results found in simulations executed by Munters and Meyers (2018), showing a potential increase in power production of up to 4%, with most of the gain coming from the first downstream turbine. Some minor differences were observed as well. First of all, the optimal Strouhal number is found to be slightly higher in the wind tunnel experiments, around $St = 0.3$. Secondly, a smaller optimal amplitude of excitation was found. This could partly be caused by a slight rotor imbalance, which resulted in significant power losses at the excited turbine. Although higher gains were observed at turbine 2, the power loss of turbine 1 could not be compensated for at higher amplitudes of excitation.

A comparison between DIC and static induction control as well as wake redirection control shows that this approach works significantly better than the former and approximately as good as the latter. This greatly strengthens the premise that DIC is an effective method to increase the power production of a wind farm as a whole.

Furthermore, by means of the aeroelastic tool CP-LAMBDA, it was shown that the effect of DIC on the Damage Equivalent Loads (DEL) of the excited wind turbine is relatively small. For the given wind ~~farm~~ turbine example, the ~~weighed~~ weighted blade root edgewise DEL was in the order of 0.3 to 0.4 % higher than in the baseline greedy control case.

In all, it can be concluded that the dynamic induction control approach shows great promise, as now both simulations and scaled experiments show that it is possible to achieve a power gain. However, ~~significant~~ some minor differences are found between simulation ~~and experiments~~studies in literature and the experiments presented here, which still need to be adressed. Future research can therefore be directed into clarifying these differences, as well as executing additional experiments, for example with different inflow velocities inside and outside the region II regime.

As the amplitude and frequency of the excitation are shown to be important control parameters, it would be a very interesting challenge to develop an algorithm that is able to optimize these parameters. Furthermore, additional analysis on the increased loads on the (downstream) turbines can be done to investigate the effect of these loads on the lifetime of turbines~~.~~, as well as the tradeoff between power and load effects. Another possible approach would be to investigate the effects of applying periodic DIC on intermediate wind turbines on the performance of the wind farm. Finally, application on full-scale wind turbines could be the last step in proving the validity of this approach.

Acknowledgements. This work has been supported by the CL-Windcon project, which receives funding from the European Union Horizon 2020 research and innovation ~~program~~ programme under grand agreement No. 727477.

References

Annoni, J., Gebraad, P. M., Scholbrock, A. K., Fleming, P. A., and Wingerden, J.-W. v.: Analysis of axial-induction-based wind plant control using an engineering and a high-order wind plant model, Wind Energy, 19, 1135–1150, 2016.

Annoni, J., Fleming, P., Scholbrock, A., Roadman, J., Dana, S., Adcock, C., Porte-Agel, F., Raach, S., Haizmann, F., and Schlipf, D.: Analysis of control-oriented wake modeling tools using lidar field results, Wind Energy Science, 3, 819–831, 2018.

Bauchau, O. A.: Flexible Multibody Dynamics, vol. 176 of *Solid Mechanics and its Applications*, Springer Netherlands, Dordrecht, Heidelberg, London, New York, https://doi.org/10.1007/978-94-007-0335-3, 2011.

Bossanyi, E.: The Design of Closed Loop Controllers for Wind Turbines, Wind Energy, 3, 149–163, 2000.

Bottasso, C. L. and Croce, A.: Cp-Lambda user manual, Tech. rep., Dipartimento di Scienze e Tecnologie Aerospaziali, Politecnico di Milano, Milano, Italy, 2009–2018.

Bottasso, C. L., Croce, A., Savini, B., Sirchi, W., and Trainelli, L.: Aero-servo-elastic modeling and control of wind turbines using finite element multibody procedures, Multibody Systems Dynamics, 16, 291–308, 2006.

Bottasso, C. L., Campagnolo, F., and Petrović, V.: Wind tunnel testing of scaled wind turbine models: Beyond aerodynamics, Journal of Wind Engineering and Industrial Aerodynamics, 127, 11–28, 2014.

Campagnolo, F., Petrović, V., Bottasso, C. L., and Croce, A.: Wind tunnel testing of wake control strategies, in: 2016 American Control Conference (ACC), pp. 513–518, 2016a.

Campagnolo, F., Petrović, V., Nanos, E., Tan, C., Bottasso, C., Paek, I., and Kim, H. K. K.: Wind tunnel testing of power maximization control strategies applied to a multi-turbine floating wind power platform, in: Proceedings of the International Offshore and Polar Engineering Conference, 2016b.

Campagnolo, F., Petrović, V., Schreiber, J., Nanos, E. M., Croce, A., and Bottasso, C. L.: Wind tunnel testing of a closed-loop wake deflection controller for wind farm power maximization, Journal of Physics: Conference Series, 753, 7, 2016c.

Churchfield, M. and Lee, S.: NWTC design codes-SOWFA, Tech. rep., National Renewable Energy Laboratory (NREL), 15013 Denver West Parkway, Golden, CO. http://wind.nrel.gov/designcodes/simulators/SOWFA, 2012.

Doekemeijer, B. M. and Storm, R.: FLORISSE_M, https://github.com/TUDelft-DataDrivenControl/FLORISSE_M, 2018.

Gebraad, P. M., van Dam, F. C., and van Wingerden, J.-W.: A model-free distributed approach for wind plant control, in: 2013 American Control Conference, pp. 628–633, IEEE, 2013.

Gebraad, P. M., Teeuwisse, F., Van Wingerden, J., Fleming, P. A., Ruben, S., Marden, J., and Pao, L.: Wind plant power optimization through yaw control using a parametric model for wake effects—a CFD simulation study, Wind Energy, 19, 95–114, 2016.

Goit, J. P. and Meyers, J.: Optimal control of energy extraction in wind-farm boundary layers, Journal of Fluid Mechanics, 768, 5–50, 2015.

Jonkman, B. J. and Buhl, M. L. J.: TurbSim user's guide, Tech. Rep. NREL/TP-500-39797, National Renewable Energy Laboratory (NREL), 15013 Denver West Parkway, Golden, CO, 2006.

Jonkman, J. M., Butterfield, S., Musial, W., and Scott, G.: Definition of a 5-MW reference wind turbine for offshore system development, Tech. Rep. NREL/TP-500-38060, National Renewable Energy Laboratory (NREL), 15013 Denver West Parkway, Golden, CO, 2009.

Marden, J. R., Ruben, S. D., and Pao, L. Y.: A model-free approach to wind farm control using game theoretic methods, IEEE Transactions on Control Systems Technology, 21, 1207–1214, 2013.

IEC 61400-1 Ed.3.: Wind Turbines — Part 1: Design requirements, Tech. rep., Garrad Hassan and Partners Ltd, St Vincent's Works, Silverthorne Lane, Bristol BS2 0QD, UK, 2004.

Munters, W. and Meyers, J.: An optimal control framework for dynamic induction control of wind farms and their interaction with the atmospheric boundary layer, Phil. Trans. R. Soc. A, 375, 20160 100, 2017.

Munters, W. and Meyers, J.: Towards practical dynamic induction control of wind farms: analysis of optimally controlled wind-farm boundary layers and sinusoidal induction control of first-row turbines, Wind Energy Science, 3, 409–425, 2018.

Nilsson, K., Ivanell, S., Hansen, K. S., Mikkelsen, R., Sørensen, J. N., Breton, S.-P., and Henningson, D.: Large-eddy simulations of the Lillgrund wind farm, Wind Energy, 18, 449–467, 2015.

Schreiber, J., Nanos, E., Campagnolo, F., and Bottasso, C. L.: Verification and calibration of a reduced order wind farm model by wind tunnel experiments, in: Journal of Physics: Conference Series, vol. 854, p. 012041, IOP Publishing, 2017.

Westergaard, C. H.: A method for improving large array wind park powre performance through active wake manipulation reducing shadow effects, 2013.